Passive Reduced-Order Models for Interconnect Simulation and their Computation via Krylov-Subspace Algorithms*

Roland W. Freund

Bell Laboratories
Lucent Technologies
Room 2C–420
700 Mountain Avenue
Murray Hill, NJ 07974–0636, USA
e-mail: freund@research.bell-labs.com

Abstract

This paper studies a general projection technique based on block Krylov subspaces for the computation of reduced-order models of multi-port RLC circuits. We show that the resulting reduced-order models are always passive, yet they still match at least half as many moments as the corresponding reduced-order models based on matrix-Padé approximation. Moreover, for the special cases of RC, RL, and LC circuits, the reduced-order models obtained by projection and by matrix-Padé approximation are identical. For general RLC circuits, we show how the projection technique can easily be incorporated into the SyMPVL algorithm to obtain passive reduced-order models, in addition to the high-accuracy matrix-Padé approximations that characterize SyMPVL, at essentially no extra computational costs. Connections between SyMPVL and the recently proposed reduced-order modeling algorithm PRIMA are also discussed. Numerical results for interconnect simulation problems are reported.

1 Introduction

Electronic circuits often contain large linear subnetworks of passive components. Such subnetworks may represent interconnect automatically extracted from layout as large RLC networks, models of IC packages, or models of wireless propagation channels. Often these linear subnetworks are so large that they need to be replaced by much smaller reduced-order models, before any numerical simulation becomes feasible. Ideally, the reduced-order models would produce a good approximation of the input-output behavior of the original linear system, at least in a limited domain of interest, e.g., a frequency range.

In recent years, reduced-order modeling techniques based on Padé approximation have been recognized to be powerful tools for various circuit simulation tasks. The first such technique was asymptotic waveform evaluation (AWE) [18, 19], which uses explicit moment

*Numerical Analysis Manuscript No. 98–3–06, Bell Laboratories, Murray Hill, New Jersey, October 1998. Available on WWW at `http://cm.bell-labs.com/cs/doc/98`.

matching. More recently, the attention has moved to reduced-order models generated by means of Krylov-subspace algorithms, which avoids the typical numerical instabilities of explicit moment matching.

PVL [7] and its multi-port version MPVL [8] use variants of the Lanczos process [15] to stably compute reduced-order models that represent Padé or matrix-Padé approximations [5] of the circuit transfer function. SyPVL [11] and its multi-port version SyMPVL [12, 13, 9] are versions of PVL and MPVL, respectively, that are tailored to RLC circuits. By exploiting the symmetry of RLC transfer functions, the computational costs of SyPVL and SyMPVL are only half of those of general PVL and MPVL. The Arnoldi process [3] is another popular Krylov-subspace algorithm. Reduced-order model techniques based on the Arnoldi process were recently proposed in [21, 16, 17, 6]. The use of congruence transforms is advocated in [14]. Arnoldi-based reduced-order models are not defined by Padé approximation, and as a result, in general, they are not as accurate as a Padé-based reduced-order model of the same size. More precisely, Arnoldi-based reduced-order models techniques are known to match only half as many moments as Lanczos-based models; see [21, 16, 17].

In many applications, in particular those related to VLSI interconnect, the reduced-order model is used as a substitute for the full-blown original model in higher-level simulations. In such applications, it is very important for the reduced-order model to maintain the passivity properties of the original circuit. In [12, 13, 4], it is shown that SyMPVL is passive for RC, RL, and LC circuits. However, the Padé-based reduced-order model that characterizes SyMPVL cannot be guaranteed to be passive for general RLC circuits. On the other hand, in [16, 17], it was proved that the Arnoldi-based reduction technique PRIMA produces passive reduced-order for general RLC circuits. PRIMA employs a block version of the Arnoldi process and then obtains reduced-order models by projecting the matrices defining the RLC transfer function onto the Arnoldi basis vectors.

In this paper, motivated by PRIMA, we introduce a general projection technique for computing reduced-order models based on block Krylov subspaces. We show that the resulting reduced-order models only depend on the underlying block Krylov subspaces, but not on the particular choice of basis vectors for these subspaces. We prove that, for RLC circuits, the reduced-order models are always passive, yet they still match at least half as many moments as the corresponding reduced-order models based on matrix-Padé approximation. We also show that for the special cases of RC, RL, and LC circuits, the reduced-order models obtained by projection and by matrix-Padé approximation are identical. For general RLC circuits, the projection technique can easily be incorporated into the SyMPVL algorithm to obtain passive reduced-order models, in addition to the high-accuracy matrix-Padé approximations that characterize SyMPVL.

The remainder of the paper is organized as follows. In Section 2, we briefly review the formulation of RLC circuit equations. In Section 3, we describe the general projection procedure for using block Krylov subspaces to generate reduced-order models and establish some basic properties. In Section 4, we prove that the reduced-order models are passive. In Section 5, we describe how the projection procedure can be incorporated into SyMPVL, and we discuss connections with PRIMA. In Section 6, numerical results for interconnect simulation problems are reported. Finally, in Section 7, we make some concluding remarks.

2 Formulation of RLC Circuit Equations

In this section, we briefly review the formulation of the circuit equations for RLC circuits.

The connectivity of a circuit can be captured using a directional graph. The nodes of the graph correspond to the nodes of the circuit, and the edges of the graph correspond to each of the circuit elements. An arbitrary direction is assigned to graph edges, so one can distinguish between the source and destination nodes. The adjacency matrix, $\mathbf{A}$, of the directional graph describes the connectivity of a circuit. Each row of the matrix corresponds to a graph edge and, therefore, to a circuit element. Each column of the matrix corresponds to a graph or circuit node. The column corresponding to the datum (ground) node of the circuit is omitted in order to remove redundancy. By convention, a row of the connectivity matrix will contain $+1$ in the column corresponding to the source node, -1 in the column corresponding to the destination node, and 0 everywhere else. It is easy to see that Kirchhoff's laws, which depend only on connectivity, can be expressed using the adjacency matrix as follows:

$$\begin{aligned} \text{KCL:} \qquad & \mathbf{A}^{\mathrm{T}}\,\mathbf{i}_b = \mathbf{0}, \\ \text{KVL:} \qquad & \mathbf{A}\,\mathbf{v}_n = \mathbf{v}_b. \end{aligned} \tag{1}$$

Here, $\mathbf{i}_b$ and $\mathbf{v}_b$ are the vectors of branch currents and voltages, respectively, and $\mathbf{v}_n$ is the vector of the non-datum node voltages.

We are interested in analyzing RLC circuits, and for simplicity, we assume that the circuit is excited just by current sources. In this case, the adjacency matrix and the branch current and voltage vectors can be partitioned according to circuit-element types as follows:

$$\mathbf{A} = \begin{bmatrix} \mathbf{A}_i \\ \mathbf{A}_g \\ \mathbf{A}_c \\ \mathbf{A}_l \end{bmatrix}, \quad \mathbf{v}_b = \begin{bmatrix} \mathbf{v}_i \\ \mathbf{v}_g \\ \mathbf{v}_c \\ \mathbf{v}_l \end{bmatrix}, \quad \mathbf{i}_b = \begin{bmatrix} \mathbf{i}_i \\ \mathbf{i}_g \\ \mathbf{i}_c \\ \mathbf{i}_l \end{bmatrix}.$$

Here, the subscripts i, g, c, and l stand for branches containing current sources, resistors, capacitors, and inductors, respectively.

The set of circuit equations is completed by adding the so-called *branch constitutive relationships* (BCR's), which describe the physical behavior of the circuit elements. In the case of RLC circuits, the BCR's are as follows:

$$\mathbf{i}_i = -\mathbf{I}_t(t), \;\; \mathbf{i}_g = \mathcal{G}\,\mathbf{v}_g, \;\; \mathbf{i}_c = \mathcal{C}\,\frac{d}{dt}\mathbf{v}_c, \;\; \mathbf{v}_l = \mathcal{L}\,\frac{d}{dt}\mathbf{i}_l. \tag{2}$$

Here, $\mathbf{I}_t(t)$ is the vector of current-source values, $\mathcal{G}$ and $\mathcal{C}$ are appropriately-sized diagonal matrices whose diagonal entries are the conductance and capacitance values of each element. It is clear that these values are positive for any physical circuit. The matrix $\mathcal{L}$ is also diagonal in the absence of inductive coupling. Inductive coupling introduces off-diagonal terms in the inductance matrix, but $\mathcal{L}$ remains symmetric and positive semi-definite.

The modified nodal formulation (MNA) of the circuit equations is obtained by combining the Kirchhoff equations (1) with the BCRs (2), and eliminating as many current unknowns as possible. For the case of RLC circuits, only inductor currents need to be left as unknowns.

Setting

$$\mathbf{G} = \begin{bmatrix} \mathbf{A}_g^{\mathrm{T}} \mathcal{G} \mathbf{A}_g & \mathbf{A}_l^{\mathrm{T}} \\ \mathbf{A}_l & \mathbf{0} \end{bmatrix}, \quad \mathbf{C} = \begin{bmatrix} \mathbf{A}_c^{\mathrm{T}} \mathcal{C} \mathbf{A}_c & \mathbf{0} \\ \mathbf{0} & -\mathcal{L} \end{bmatrix},$$
$$\mathbf{x} = \begin{bmatrix} \mathbf{v}_n \\ \mathbf{i}_l \end{bmatrix}, \quad \mathbf{B} = \begin{bmatrix} \mathbf{A}_i^{\mathrm{T}} \\ \mathbf{0} \end{bmatrix}, \tag{3}$$

the resulting MNA equations can be written compactly in matrix form as follows:

$$\mathbf{G}\,\mathbf{x} + \mathbf{C}\,\frac{d}{dt}\mathbf{x} = \mathbf{B}\,\mathbf{I}_t(t). \tag{4}$$

Note that the matrices $\mathbf{G}$ and $\mathbf{C}$ in (3) are symmetric. They are however indefinite in general.

We are interested in determining the network functions of the RLC block viewed as an m-terminal component. Since we allowed only current sources in our formulation, it is natural to determine the matrix $\mathbf{Z}(s)$ of $\mathbf{Z}$-parameters. By applying the Laplace transform to (4) and assuming zero initial conditions, we obtain

$$\begin{aligned} (\mathbf{G} + s\,\mathbf{C})\,\mathbf{X} &= \mathbf{B}\,\mathbf{I}_s(s), \\ \mathbf{V}_i &= \mathbf{B}^{\mathrm{T}}\,\mathbf{X}. \end{aligned} \tag{5}$$

Here, $\mathbf{X}$, $\mathbf{I}_s(s)$, and $\mathbf{V}_i$ represent the Laplace transforms of the unknown vector $\mathbf{x}$, the excitation current $\mathbf{I}_t(t)$, and the vector of voltages across the excitation sources, respectively. Eliminating $\mathbf{X}$ in (5) gives

$$\begin{aligned} \mathbf{V}_i = \begin{bmatrix} \mathbf{A}_i & \mathbf{0} \end{bmatrix} \mathbf{X} &= \mathbf{Z}(s)\,\mathbf{I}_s(s), \\ \text{where} \quad \mathbf{Z}(s) &= \mathbf{B}^{\mathrm{T}}\,(\mathbf{G} + s\,\mathbf{C})^{-1}\,\mathbf{B}. \end{aligned} \tag{6}$$

Here, $\mathbf{G}$ and $\mathbf{C}$ are real symmetric $N \times N$ matrices, and $\mathbf{B}$ is a real $N \times m$ matrix. For general RLC circuits, $\mathbf{G}$ and $\mathbf{C}$ are indefinite. In the important special cases of RC and RL circuits, the formulation can be modified such that the matrices $\mathbf{G}$ and $\mathbf{C}$ in (6) are positive semi-definite. For LC circuits, the formulation can be modified such that

$$\mathbf{Z}(s) = \mathbf{B}^{\mathrm{T}}\left(\mathbf{G} + s^2\,\mathbf{C}\right)^{-1}\mathbf{B}, \tag{7}$$

where again $\mathbf{G}$ and $\mathbf{C}$ are positive semi-definite.

For the general case of RLC circuits, we will also use the following reformulation of $\mathbf{Z}$. Let $\mathbf{J}$ be the block matrix

$$\mathbf{J} = \begin{bmatrix} \mathbf{I} & \mathbf{0} \\ \mathbf{0} & -\mathbf{I} \end{bmatrix}, \tag{8}$$

where $\mathbf{I}$ denotes the identity matrix and the sizes of the blocks in (8) are the same as in the partitioning of $\mathbf{G}$ and $\mathbf{C}$ in (3). Note that, by (3) and (8), we have $\mathbf{B} = \mathbf{J}\,\mathbf{B}$. Using this relation, we can rewrite the formula (6) as follows:

$$\mathbf{Z}(s) = \mathbf{B}^{\mathrm{T}}\,(\mathbf{J}\,\mathbf{G} + s\,\mathbf{J}\,\mathbf{C})^{-1}\,\mathbf{B}. \tag{9}$$

Here, by (3) and (8), the matrices $\mathbf{J}\,\mathbf{G}$ and $\mathbf{J}\,\mathbf{C}$ are of the form

$$\mathbf{J}\,\mathbf{G} = \begin{bmatrix} \mathbf{A}_g^{\mathrm{T}} \mathcal{G} \mathbf{A}_g & \mathbf{A}_l^{\mathrm{T}} \\ -\mathbf{A}_l & \mathbf{0} \end{bmatrix} \quad \text{and} \quad \mathbf{J}\,\mathbf{C} = \begin{bmatrix} \mathbf{A}_c^{\mathrm{T}} \mathcal{C} \mathbf{A}_c & \mathbf{0} \\ \mathbf{0} & \mathcal{L} \end{bmatrix}. \tag{10}$$

In this formulation, the matrix $\mathbf{J}\,\mathbf{G}$ is no longer symmetric, however, the matrix $\mathbf{J}\,\mathbf{C}$ is symmetric positive semi-definite.

3 Reduced-Order Models via Projection

In this section, we consider general m-input p-output transfer functions of the form

$$\mathbf{Z}(s) = \mathbf{L}^{\mathrm{H}} \left(\mathbf{G} + s\,\mathbf{C}\right)^{-1} \mathbf{B}, \tag{11}$$

where $\mathbf{G}$ and $\mathbf{C}$ are $N \times N$ matrices, $\mathbf{B}$ is an $N \times m$, and $\mathbf{L}$ is an $N \times p$ matrix. The matrices $\mathbf{G}$, $\mathbf{C}$, $\mathbf{B}$, and $\mathbf{L}$ are allowed to have complex entries, and in (11), $\mathbf{L}^{\mathrm{H}} = \left[\overline{l_{kj}}\right]$ denotes the complex-conjugate transpose of $\mathbf{L} = \left[l_{jk}\right]$. The only assumption we make is that $\mathbf{G} + s\,\mathbf{C}$ is a regular matrix pencil. This means that the matrix $\mathbf{G} + s\,\mathbf{C}$ is singular only for finitely many values of $s \in \mathbb{C}$. Note that the s's for which $\mathbf{G} + s\,\mathbf{C}$ is singular are just the poles of the function (11). Clearly, RLC transfer functions of the form (6) are a special case of (11) with $\mathbf{L} = \mathbf{B}$ and real matrices $\mathbf{G}$, $\mathbf{C}$, and $\mathbf{B}$.

3.1 Block Krylov Subspaces

Let $s_0 \in \mathbb{C}$ be an arbitrarily chosen expansion point such that the matrix $\mathbf{G} + s_0\,\mathbf{C}$ is nonsingular. We can then rewrite (11) as follows:

$$\begin{aligned} \mathbf{Z}(s) &= \mathbf{L}^{\mathrm{H}} \left(\mathbf{G} + s_0\,\mathbf{C} + (s - s_0)\;\mathbf{C}\right)^{-1} \mathbf{B} \\ &= \mathbf{L}^{\mathrm{H}} \left(\mathbf{I} + (s - s_0)\;\mathbf{A}\right)^{-1} \mathbf{R}. \end{aligned} \tag{12}$$

Here, $\mathbf{I}$ denotes the $N \times N$ identity matrix, and $\mathbf{A}$ and $\mathbf{R}$ are given by

$$\mathbf{A} = \left(\mathbf{G} + s_0\,\mathbf{C}\right)^{-1} \mathbf{C} \quad \text{and} \quad \mathbf{R} = \left(\mathbf{G} + s_0\,\mathbf{C}\right)^{-1} \mathbf{B}. \tag{13}$$

We will use block Krylov subspaces induced by the matrices (13) to generate reduced-order models for (11). Next, we briefly review the notion of block Krylov subspaces; see [1] for details.

The matrix sequence

$$\mathbf{R}, \mathbf{A}\,\mathbf{R}, \mathbf{A}^2\,\mathbf{R}, \ldots, \mathbf{A}^{q-1}\,\mathbf{R}, \ldots \tag{14}$$

is called a *block Krylov sequence*. The columns of the matrices in (14) are vectors of length N, and thus at most N of these columns are linearly independent. By scanning the columns of the matrices in (14) from left to right and deleting each column that is linearly dependent on earlier columns, we obtain the *deflated* block Krylov sequence

$$\mathbf{R}_1, \mathbf{A}\,\mathbf{R}_2, \mathbf{A}^2\,\mathbf{R}_3, \ldots, \mathbf{A}^{q_{\max}-1}\,\mathbf{R}_{q_{\max}}. \tag{15}$$

This process of deleting linearly dependent vectors is referred to as *deflation* in the following. In (15), for each $q = 1, 2, \ldots, q_{\max}$, $\mathbf{R}_q$ is a submatrix of $\mathbf{R}_{q-1}$, with $\mathbf{R}_q \neq \mathbf{R}_{q-1}$ if, and only if, deflation occurred within the q-th Krylov block $\mathbf{A}^{q-1}\mathbf{R}$ in (14). Here, for $q = 1$, we set $\mathbf{R}_0 = \mathbf{R}$. Denoting by m_q the number of columns of $\mathbf{R}_q$, we thus have

$$m \geq m_1 \geq m_2 \geq \cdots \geq m_{q_{\max}} \geq 1. \tag{16}$$

By construction the columns of the matrices (15) are linearly independent, and for each n, the subspace spanned by the first n of these columns is called the *n-th block Krylov subspace* (induced by $\mathbf{A}$ and $\mathbf{R}$). In the following, we denote the n-th block Krylov subspace by $\mathcal{K}_n(\mathbf{A}, \mathbf{R})$. For later use, we state the following invariance property of block Krylov subspaces.

Lemma 1 *Let $\mathbf{J}$ be any nonsingular $N \times N$ matrix. Then the matrix triplets $\mathbf{G}$, $\mathbf{C}$, $\mathbf{B}$ and $\mathbf{J}\,\mathbf{G}$, $\mathbf{J}\,\mathbf{C}$, $\mathbf{J}\,\mathbf{B}$ lead to the same n-th block Krylov subspace $\mathcal{K}_n(\mathbf{A}, \mathbf{R})$.*

Proof By (13), we have

$$\begin{aligned}
\mathbf{A} &= (\mathbf{G} + s_0\,\mathbf{C})^{-1}\,\mathbf{C} = (\mathbf{J}\,\mathbf{G} + s_0\,\mathbf{J}\,\mathbf{C})^{-1}\,\mathbf{J}\,\mathbf{C}, \\
\mathbf{R} &= (\mathbf{G} + s_0\,\mathbf{C})^{-1}\,\mathbf{B} = (\mathbf{J}\,\mathbf{G} + s_0\,\mathbf{J}\,\mathbf{C})^{-1}\,\mathbf{J}\,\mathbf{B}.
\end{aligned}$$

Thus both matrix triplets result in the same matrices $\mathbf{A}$ and $\mathbf{R}$ and the associated block Krylov subspaces are identical. $\square$

In the following, we always assume that $1 \leq q \leq q_{\max}$ is arbitrary, and we set

$$n = m_1 + m_2 + \cdots + m_q. \tag{17}$$

Note that, by (16), $n \leq m \cdot q$ with $n = m \cdot q$ if no deflation has occurred. By construction, the n-th block Krylov subspace is then given by

$$\mathcal{K}_n(\mathbf{A}, \mathbf{R}) = \operatorname{colspan}\{\mathbf{R}_1, \mathbf{A}\,\mathbf{R}_2, \ldots, \mathbf{A}^{q-1}\,\mathbf{R}_q\}. \tag{18}$$

3.2 Reduced-Order Models

By simply projecting the matrices $\mathbf{G}$, $\mathbf{C}$, $\mathbf{B}$, $\mathbf{L}$ onto the n-th block Krylov subspace, one obtains a reduced-order model, $\mathbf{Z}_n$, of the transfer function (11). To this end, we choose any set of vectors,

$$\mathbf{v}_1, \mathbf{v}_2, \ldots, \mathbf{v}_n, \tag{19}$$

that span the n-th block Krylov subspace (18), i.e.,

$$\operatorname{span}\{\mathbf{v}_1, \mathbf{v}_2, \ldots, \mathbf{v}_n\} = \mathcal{K}_n(\mathbf{A}, \mathbf{R}). \tag{20}$$

Moreover, we denote by

$$\mathbf{V}_n = \begin{bmatrix} \mathbf{v}_1 & \mathbf{v}_2 & \cdots & \mathbf{v}_n \end{bmatrix} \tag{21}$$

the $N \times n$ matrix whose columns are the basis vectors (19). The reduced-order model $\mathbf{Z}_n$ of (11) is then given by

$$\mathbf{Z}_n(s) = \mathbf{L}_n^{\mathrm{H}} \left(\mathbf{G}_n + s\, \mathbf{C}_n\right)^{-1} \mathbf{B}_n, \tag{22}$$

where

$$\mathbf{G}_n = \mathbf{V}_n^{\mathrm{H}}\, \mathbf{G}\, \mathbf{V}_n, \quad \mathbf{C}_n = \mathbf{V}_n^{\mathrm{H}}\, \mathbf{C}\, \mathbf{V}_n, \quad \mathbf{B}_n = \mathbf{V}_n^{\mathrm{H}}\, \mathbf{B}, \quad \text{and} \quad \mathbf{L}_n = \mathbf{V}_n^{\mathrm{H}}\, \mathbf{L}. \tag{23}$$

While the reduced-order transfer function $\mathbf{Z}_n$ is defined via the basis vectors (19), it turns out that $\mathbf{Z}_n$ does not depend on the particular choice of the basis vectors.

Theorem 1 *The reduced-order transfer function $\mathbf{Z}_n$ given by* (22) *and* (23) *does not depend on the particular choice of the basis vectors, $\mathbf{v}_1, \mathbf{v}_2, \ldots, \mathbf{v}_n$, for the n-th block Krylov subspace $\mathcal{K}_n(\mathbf{A}, \mathbf{R})$.*

Proof Let (19) be the basis vectors used in (22) and (23). Let $\widetilde{\mathbf{v}}_1, \widetilde{\mathbf{v}}_2, \ldots, \widetilde{\mathbf{v}}_n$ be any other set of vectors that span $\mathcal{K}_n(\mathbf{A}, \mathbf{R})$, and set $\widetilde{\mathbf{V}}_n = \begin{bmatrix} \widetilde{\mathbf{v}}_1 & \widetilde{\mathbf{v}}_2 & \cdots & \widetilde{\mathbf{v}}_n \end{bmatrix}$. In analogy to (22) and (23), the matrix $\widetilde{\mathbf{V}}_n$ leads to the reduced-order transfer function

$$\widetilde{\mathbf{Z}}_n(s) = \widetilde{\mathbf{L}}_n^{\mathrm{H}} \left(\widetilde{\mathbf{G}}_n + s\, \widetilde{\mathbf{C}}_n\right)^{-1} \widetilde{\mathbf{B}}_n, \tag{24}$$

where

$$\widetilde{\mathbf{G}}_n = \widetilde{\mathbf{V}}_n^{\mathrm{H}}\, \mathbf{G}\, \widetilde{\mathbf{V}}_n, \quad \widetilde{\mathbf{C}}_n = \widetilde{\mathbf{V}}_n^{\mathrm{H}}\, \mathbf{C}\, \widetilde{\mathbf{V}}_n, \quad \widetilde{\mathbf{B}}_n = \widetilde{\mathbf{V}}_n^{\mathrm{H}}\, \mathbf{B}, \quad \text{and} \quad \widetilde{\mathbf{L}}_n = \widetilde{\mathbf{V}}_n^{\mathrm{H}}\, \mathbf{L}. \tag{25}$$

Since the columns of both matrices $\mathbf{V}_n$ and $\widetilde{\mathbf{V}}_n$ span the same subspace, there exists a nonsingular $n \times n$ matrix $\mathbf{M}$ such that $\widetilde{\mathbf{V}}_n = \mathbf{V}_n\, \mathbf{M}$. Using this relation, we obtain from (25) and (23) that

$$\widetilde{\mathbf{G}}_n = \mathbf{M}^{\mathrm{H}}\, \mathbf{G}_n\, \mathbf{M}, \quad \widetilde{\mathbf{C}}_n = \mathbf{M}^{\mathrm{H}}\, \mathbf{C}_n\, \mathbf{M}, \quad \widetilde{\mathbf{B}}_n = \mathbf{M}^{\mathrm{H}}\, \mathbf{B}_n, \quad \text{and} \quad \widetilde{\mathbf{L}}_n = \mathbf{M}^{\mathrm{H}}\, \mathbf{L}_n. \tag{26}$$

Inserting (26) into (24), we get

$$\begin{aligned} \widetilde{\mathbf{Z}}_n(s) &= \mathbf{L}_n^{\mathrm{H}}\, \mathbf{M} \left(\mathbf{M}^{\mathrm{H}} \left(\mathbf{G}_n + s\, \mathbf{C}_n\right) \mathbf{M}\right)^{-1} \mathbf{M}^{\mathrm{H}}\, \mathbf{B}_n \\ &= \mathbf{L}_n^{\mathrm{H}} \left(\mathbf{G}_n + s\, \mathbf{C}_n\right)^{-1} \mathbf{B}_n. \end{aligned} \tag{27}$$

Thus, by (22) and (27), the reduced-order transfer functions $\mathbf{Z}_n$ and $\widetilde{\mathbf{Z}}_n$ are identical. $\square$

3.3 Moment Matching

Although the reduced-order transfer function $\mathbf{Z}_n$ is defined by a simple projection, $\mathbf{Z}_n$ satisfies a moment-matching property. For the special case of expansion point $s_0 = 0$ and basis vectors generated by block Arnoldi without deflation, the moment-matching property was first observed in [16]. Here we extend this result to the most general case where possibly nonzero expansion points s_0 are allowed and where the underlying block Krylov subspaces allow the necessary deflation of linearly dependent vectors.

By (12), expanding the transfer function $\mathbf{Z}$ about s_0 yields

$$\mathbf{Z}(s) = \sum_{i=0}^{\infty} (-1)^i \, \mathbf{M}_i \, (s - s_0)^i, \quad \text{where} \quad \mathbf{M}_i = \mathbf{L}^{\mathrm{T}} \, \mathbf{A}^i \, \mathbf{R}. \tag{28}$$

On the other hand, expanding the reduced-order transfer function (22) about s_0 gives

$$\mathbf{Z}_n(s) = \sum_{i=0}^{\infty} (-1)^i \, \widehat{\mathbf{M}}_i \, (s - s_0)^i, \tag{29}$$

where

$$\widehat{\mathbf{M}}_i = \mathbf{L}_n^{\mathrm{T}} \left(\left(\mathbf{G}_n + s_0 \, \mathbf{C}_n \right)^{-1} \mathbf{C}_n \right)^i \left(\mathbf{G}_n + s_0 \, \mathbf{C}_n \right)^{-1} \mathbf{B}_n \quad \text{for all} \quad i. \tag{30}$$

It turns out that the first q terms in the expansions (28) and (30) are identical.

Theorem 2 *Let $n = m_1 + m_2 + \cdots + m_q$. Then, the first q moments $\mathbf{M}_i$ and $\widehat{\mathbf{M}}_i$ in the expansions* (28) *and* (30) *of $\mathbf{Z}$ and $\mathbf{Z}_n$ are identical :*

$$\mathbf{M}_i = \widehat{\mathbf{M}}_i \quad \textit{for all} \quad i = 0, 1, \ldots, q - 1. \tag{31}$$

Proof Let $\mathbf{F}$ be the $N \times N$ matrix defined by

$$\mathbf{F} = \mathbf{V}_n \, \left(\mathbf{G}_n + s_0 \, \mathbf{C}_n \right)^{-1} \mathbf{V}_n^{\mathrm{T}} \, \mathbf{C}. \tag{32}$$

In the Appendix, we show that, in terms of $\mathbf{F}$, the moments $\widehat{\mathbf{M}}_i$ of $\mathbf{Z}_n$ have the following representation:

$$\widehat{\mathbf{M}}_i = \mathbf{L}^{\mathrm{T}} \, \mathbf{F}^i \, \mathbf{R} \quad \text{for all} \quad i \geq 0. \tag{33}$$

Furthermore, in the Appendix, we prove that

$$\mathbf{F}^i \, \mathbf{R} = \mathbf{A}^i \, \mathbf{R} \quad \text{for all} \quad i = 0, 1, \ldots, q - 1. \tag{34}$$

Inserting (34) into (33) gives

$$\widehat{\mathbf{M}}_i = \mathbf{L}^{\mathrm{T}} \, \mathbf{F}^i \, \mathbf{R} = \mathbf{L}^{\mathrm{T}} \, \mathbf{A}^i \, \mathbf{R} = \mathbf{M}_i \quad \text{for all} \quad i = 0, 1, \ldots, q - 1,$$

which is the desired moment-matching property (31). $\square$

4 Passivity

We now return to the RLC transfer functions $\mathbf{Z}$ described in Section 2. Recall that $\mathbf{Z}$ is defined by (6) with matrices $\mathbf{G}$, $\mathbf{C}$, and $\mathbf{B}$ given by (3), and that (9) is an equivalent representation of $\mathbf{Z}$. From now on, we assume that a real expansion point s_0 is chosen.

It is well known (see, e.g., [23, 2]) that a transfer function $\mathbf{Z}$ is *passive* if, and only if, the following three conditions are satisfied:

(i) $\mathbf{Z}(s)$ has no poles in $\mathbb{C}_+ = \{\, s \in \mathbb{C} \mid \operatorname{Re} s > 0 \,\}$ (the right half of the complex plane);

(ii) $\mathbf{Z}(\bar{s}) = \overline{\mathbf{Z}(s)}$ for all $s \in \mathbb{C}$;

(iii) $\operatorname{Re}\left(\mathbf{x}^{\mathrm{H}}\, \mathbf{Z}(s)\, \mathbf{x}\right) \geq 0$ for all $s \in \mathbb{C}_+$ and $\mathbf{x} \in \mathbb{C}^m$.

In particular, RLC transfer functions $\mathbf{Z}$ are passive. In this section, we show that the reduced-order transfer function $\mathbf{Z}_n$ obtained by projecting $\mathbf{Z}$ onto the n-th block Krylov subspace $\mathcal{K}_n(\mathbf{A}, \mathbf{R})$ inherits the passivity of $\mathbf{Z}$. Here, the projection is done based on the representation (9) of $\mathbf{Z}$. In view of (13), the matrices $\mathbf{A}$ and $\mathbf{R}$ are real, and let (19) be any set of real vectors that span $\mathcal{K}_n(\mathbf{A}, \mathbf{R})$. Let $\mathbf{V}_n$ be the associated real matrix defined by (21). Then, applying the projection procedure (22) and (23) to the representation (9) of $\mathbf{Z}$, we obtain the reduced-order transfer function

$$
\begin{aligned}
&\mathbf{Z}_n(s) = \mathbf{B}_n^{\mathrm{T}}\, \left(\mathbf{G}_n + s\, \mathbf{C}_n\right)^{-1} \mathbf{B}_n, \\
&\text{where} \quad \mathbf{G}_n = \mathbf{V}_n^{\mathrm{T}}\, \mathbf{J}\, \mathbf{G}\, \mathbf{V}_n, \quad \mathbf{C}_n = \mathbf{V}_n^{\mathrm{T}}\, \mathbf{J}\, \mathbf{C}\, \mathbf{V}_n, \quad \mathbf{B}_n = \mathbf{V}_n^{\mathrm{T}}\, \mathbf{B}.
\end{aligned}
\tag{35}
$$

Theorem 3 *The reduced-order model transfer function* $\mathbf{Z}_n$ *given by* (35) *is passive.*

Proof We need to show that $\mathbf{Z}_n$ satisfies conditions (i), (ii), and (iii) for passivity given above.

Condition (ii) follows directly from the fact that the matrices $\mathbf{G}_n$, $\mathbf{C}_n$, and $\mathbf{B}_n$ in the definition (35) of $\mathbf{Z}_n$ are real.

Next, we verify condition (iii). Let $s = s_1 + \mathrm{j}\, s_2 \in \mathbb{C}_+$ be arbitrary, but fixed. Here $\mathrm{j} = \sqrt{-1}$ denotes the purely imaginary unit. In the sequel, we denote the $(1,1)$-subblocks of the matrices $\mathbf{J}\, \mathbf{G}$ and $\mathbf{J}\, \mathbf{C}$ in (10) by $\mathbf{N} = \mathbf{A}_g^{\mathrm{T}} \mathcal{G} \mathbf{A}_g$ and $\mathbf{Q} = \mathbf{A}_c^{\mathrm{T}} \mathcal{C} \mathbf{A}_c$. By (10), we have

$$
\begin{aligned}
&\left(\mathbf{J}\, \mathbf{G} + s\, \mathbf{J}\, \mathbf{C}\right)^{\mathrm{H}} = \mathbf{M} + \mathbf{S}, \\
&\text{where} \quad \mathbf{M} = \begin{bmatrix} \mathbf{N} + s_1\, \mathbf{Q} & \mathbf{0} \\ \mathbf{0} & s_1\, \mathcal{L} \end{bmatrix}, \quad \mathbf{S} = \begin{bmatrix} -s_2\, \mathrm{j}\, \mathbf{Q} & -\mathbf{A}_l^{\mathrm{T}} \\ \mathbf{A}_l & -s_2\, \mathrm{j}\, \mathcal{L} \end{bmatrix}.
\end{aligned}
\tag{36}
$$

Recall that $\mathbf{N}$, $\mathbf{Q}$, and $\mathcal{L}$ are real symmetric positive semi-definite matrices and that $s_1 = \operatorname{Re} s > 0$. This guarantees that $\mathbf{M}$ is also a real symmetric positive semi-definite matrix. Similarly, the matrix $\mathbf{S}$ is complex and skew-Hermitian, i.e., $\mathbf{S} = -\mathbf{S}^{\mathrm{H}}$. These properties of $\mathbf{M}$ and $\mathbf{S}$ imply that

$$
\mathbf{y}^{\mathrm{H}}\, \mathbf{M}\, \mathbf{y} = \operatorname{Re}\left(\mathbf{y}^{\mathrm{H}}\, \mathbf{M}\, \mathbf{y}\right) \geq 0 \quad \text{and} \quad \operatorname{Re}\left(\mathbf{y}^{\mathrm{H}}\, \mathbf{S}\, \mathbf{y}\right) = 0 \quad \text{for all} \quad \mathbf{y} \in \mathbb{C}^n. \tag{37}
$$

From (36) and (37), it follows that

$$
\operatorname{Re}\left(\mathbf{y}^{\mathrm{H}}\, \left(\mathbf{J}\, \mathbf{G} + s\, \mathbf{J}\, \mathbf{C}\right)^{\mathrm{H}}\, \mathbf{y}\right) = \operatorname{Re}\left(\mathbf{y}^{\mathrm{H}}\, \mathbf{M}\, \mathbf{y}\right) \geq 0 \quad \text{for all} \quad \mathbf{y} \in \mathbb{C}^n. \tag{38}
$$

We now assume that the complex number $s \in \mathbb{C}_+$ is not an eigenvalue of the matrix pencil $\mathbf{G}_n + s\, \mathbf{C}_n$, i.e., the matrix $\mathbf{G}_n + s\, \mathbf{C}_n$ is nonsingular. Furthermore, let $\mathbf{x} \in \mathbb{C}^m$ be arbitrary, and set

$$
\mathbf{y} = \mathbf{V}_n\, \left(\mathbf{G}_n + s\, \mathbf{C}_n\right)^{-1} \mathbf{B}_n\, \mathbf{x}. \tag{39}
$$

Note that, by (35), we have

$$\mathbf{G}_n + s\,\mathbf{C}_n = \mathbf{V}_n^{\mathrm{T}}\,(\mathbf{J}\,\mathbf{G} + s\,\mathbf{J}\,\mathbf{C})\,\mathbf{V}_n. \tag{40}$$

Using (35), (39), and (40), we obtain

$$\begin{aligned}\mathbf{x}^{\mathrm{H}}\,\mathbf{Z}_n(s)\,\mathbf{x} &= \mathbf{x}^{\mathrm{H}}\,\mathbf{B}_n^{\mathrm{T}}\,\left(\mathbf{G}_n + s\,\mathbf{C}_n\right)^{-1}\mathbf{B}_n\,\mathbf{x} \\ &= \mathbf{x}^{\mathrm{H}}\,\mathbf{B}_n^{\mathrm{T}}\,\left(\mathbf{G}_n + s\,\mathbf{C}_n\right)^{-\mathrm{H}}\left(\mathbf{G}_n + s\,\mathbf{C}_n\right)^{\mathrm{H}}\left(\mathbf{G}_n + s\,\mathbf{C}_n\right)^{-1}\,\mathbf{B}_n\,\mathbf{x} \\ &= \Big(\left(\mathbf{G}_n + s\,\mathbf{C}_n\right)^{-1}\,\mathbf{B}_n\,\mathbf{x}\Big)^{\mathrm{H}}\,\left(\mathbf{G}_n + s\,\mathbf{C}_n\right)^{\mathrm{H}}\,\Big(\left(\mathbf{G}_n + s\,\mathbf{C}_n\right)^{-1}\,\mathbf{B}_n\,\mathbf{x}\Big) \\ &= \mathbf{y}^{\mathrm{H}}\,\left(\mathbf{G}_n + s\,\mathbf{C}_n\right)^{\mathrm{H}}\,\mathbf{y}.\end{aligned} \tag{41}$$

Combining (38) and (41), it follows that

$$\mathrm{Re}\left(\mathbf{x}^{\mathrm{H}}\,\mathbf{Z}_n(s)\,\mathbf{x}\right) = \mathrm{Re}\left(\mathbf{y}^{\mathrm{H}}\,\left(\mathbf{G}_n + s\,\mathbf{C}_n\right)^{\mathrm{H}}\,\mathbf{y}\right) \geq 0 \quad \text{for all} \quad \mathbf{x} \in \mathbb{C}^m \tag{42}$$

and for all $s \in \mathbb{C}_+$ for which $\mathbf{G}_n + s\,\mathbf{C}_n$ is nonsingular. Now let $\hat{s} \in \mathbb{C}_+$ be such that $\mathbf{G}_n + \hat{s}\,\mathbf{C}_n$ is singular. Note that there are at most n such "singular" points $\hat{s}$. Therefore, each $\hat{s}$ is an isolated point in $\mathbb{C}_+$, i.e., there exists an $\epsilon = \epsilon(\hat{s}) > 0$ and a neighborhood

$$N_\epsilon = \{\, s \in \mathbb{C} \mid 0 < |s - \hat{s}| \leq \epsilon \,\}$$

of $\hat{s}$ such that $N_\epsilon \subset \mathbb{C}_+$ and $\mathbf{G}_n + s\,\mathbf{C}_n$ is nonsingular for all $s \in N_\epsilon$. Thus (42) holds true for all $s \in N_\epsilon$. If the number $\hat{s}$ is not a pole of the matrix rational function $\mathbf{Z}_n$, then $\mathbf{Z}_n(\hat{s}) = \lim_{s\to\hat{s}} \mathbf{Z}_n(s)$ is a finite matrix. In this case, by taking limits $s \to \hat{s}$ in (42), it follows that (42) also holds true for $s = \hat{s}$. Now suppose that $\hat{s}$ is a pole of $\mathbf{Z}_n$. Then at least one of the entries $z_{jk}(s)$ of $\mathbf{Z}_n(s) = \left[z_{jk}(s)\right]_{1\leq j,k\leq n}$ has a pole at $\hat{s}$. and hence z_{jk} maps N_ϵ onto a suitable neighborhood of ∞ in the complex plane. Such an $z_{jk}(s)$ maps N_ϵ onto a suitable neighborhood of ∞ in the complex plane and, in particular, attains large negative numbers in N_ϵ. By selecting a suitable entry z_{jk} of $\mathbf{Z}_n$ and an associated vector $\mathbf{x} \in \mathbb{C}^m$, it is thus possible to find a point $s \in N_\epsilon$ such that $\mathrm{Re}\left(\mathbf{x}^{\mathrm{H}}\mathbf{Z}_n(s)\,\mathbf{x}\right) < 0$. However, this is a contraction to (42), and therefore, $\hat{s}$ cannot be a pole of $\mathbf{Z}_n$. This concludes the proof of (iii).

It remains to verify condition (i). By (35), if $\hat{s}$ is a pole of $\mathbf{Z}_n$, then the matrix $\mathbf{G}_n + \hat{s}\,\mathbf{C}_n$ is necessarily singular, i.e., $\hat{s}$ is a singular point. However, we have just shown that there are no such singular points $\hat{s} \in \mathbb{C}_+$. Consequently, $\mathbf{Z}_n$ cannot have poles in $\mathbb{C}_+$.

The matrix function $\mathbf{Z}_n$ satisfies all three conditions (i)–(iii), and hence the reduced-order model given by $\mathbf{Z}_n$ is passive. $\square$

5 Reduced-Order Models generated from SyMPVL

In this section, we discuss the generation of reduced-order models from SyMPVL.

5.1 Review of SyMPVL

SyMPVL is applied to the "symmetric" representation (6) of the RLC transfer function $\mathbf{Z}$. Recall that the matrices $\mathbf{G}$ and $\mathbf{C}$ in (6) are symmetric. SyMPVL exploits this symmetry by using a symmetric Lanczos-type algorithm to generate basis vectors (19) for the n-th block Krylov subspace $\mathcal{K}_n(\mathbf{A}, \mathbf{R})$. By exploiting this symmetry, the computational cost of n steps of SyMPVL is half of that of n steps of the more general MPVL method.

The symmetric Lanczos-type algorithm constructs basis vectors that are orthogonal with respect to the symmetric matrix $\mathbf{G} + s_0\,\mathbf{C}$, i.e.,

$$\mathbf{v}_j^{\mathrm{T}}\ (\mathbf{G} + s_0\,\mathbf{C})\ \mathbf{v}_k = \begin{cases} \delta_j & \text{if } j = k, \\ 0 & \text{if } j \neq k, \end{cases} \qquad \text{for all} \quad j, k = 1, 2, \ldots, n. \tag{43}$$

Using the matrix $\mathbf{V}_n$ defined in (21), we can rewrite the orthogonality conditions (43) in compact matrix form as follows:

$$\mathbf{V}_n^{\mathrm{T}}\ (\mathbf{G} + s_0\,\mathbf{C})\ \mathbf{V}_n = \boldsymbol{\Delta}_n = \operatorname{diag}(\delta_1, \delta_2, \ldots, \delta_n). \tag{44}$$

The recurrence coefficients used to generate the basis vectors (19) define an $n \times n$ matrix $\mathbf{T}_n$. The entries of $\mathbf{T}_n$ can either be generated directly (see [12, 13]), or by employing coupled recurrences to first compute a suitable factorization of $\mathbf{T}_n$ (see [4]). The matrix $\mathbf{T}_n$ can be interpreted as a certain projection of the matrix $\mathbf{A}$ defined in (13) onto the n-dimensional subspace $\mathcal{K}_n(\mathbf{A}, \mathbf{B})$. From this projection property, it can be shown that

$$\mathbf{T}_n = \boldsymbol{\Delta}_n^{-1}\,\mathbf{V}_n^{\mathrm{T}}\,\mathbf{C}\,\mathbf{V}_n. \tag{45}$$

The first m_1 vectors in (19) are obtained by orthogonalizing (with respect to $\mathbf{G} + s_0\,\mathbf{C}$) the columns of $\mathbf{R}$. We denote by $\boldsymbol{\rho}$ the $m_1 \times m$ matrix whose entries are the recurrence coefficients used in this orthogonalization process. We thus have the relation $\mathbf{V}_{m_1}\,\boldsymbol{\rho} = \mathbf{R}$, which, for $n \geq m_1$, we can rewrite as follows:

$$\mathbf{V}_n\,\boldsymbol{\rho}_n = \mathbf{R}, \quad \text{where} \quad \boldsymbol{\rho}_n = \begin{bmatrix} \boldsymbol{\rho} \\ \mathbf{0} \end{bmatrix}. \tag{46}$$

By multiplying (46) from the left by $\mathbf{V}_n^{\mathrm{T}}\ (\mathbf{G} + s_0\,\mathbf{C})$ and using (44), as well as the definition of $\mathbf{R}$ in (13), we obtain the relation

$$\boldsymbol{\Delta}_n\,\boldsymbol{\rho}_n = \mathbf{V}_n^{\mathrm{T}}\ (\mathbf{G} + s_0\,\mathbf{C})\ \mathbf{R} = \mathbf{V}_n^{\mathrm{T}}\,\mathbf{B}. \tag{47}$$

5.2 Two Reduced-Order Models

As in (17), we now assume that $n = m_1 + m_2 + \cdots + m_q$, where $1 \leq q \leq q_{\max}$. After n steps of the underlying Lanczos-type algorithm, SyMPVL produces an *n-th matrix-Padé approximant*, $\mathbf{Z}_n^{(\text{Padé})}$, to the transfer function $\mathbf{Z}$. More precisely, $\mathbf{Z}_n^{(\text{Padé})}$ is given by

$$\mathbf{Z}_n^{(\text{Padé})}(s) = (\boldsymbol{\Delta}_n\,\boldsymbol{\rho}_n)^{\mathrm{T}}\ \left(\mathbf{I} + (s - s_0)\,\mathbf{T}_n\,\right)^{-1}\ \boldsymbol{\rho}_n, \tag{48}$$

where $\mathbf{T}_n$, $\mathbf{\Delta}_n$, and $\boldsymbol{\rho}_n$ are the matrices introduced in the previous section. In [10, 13], it was shown that $\mathbf{Z}_n^{(\mathrm{Padé})}$ matches the first $2q$ moments of $\mathbf{Z}$ about the expansion point s_0, i.e.,

$$\mathbf{Z}_n^{(\mathrm{Padé})}(s) = \mathbf{Z}(s) + \mathcal{O}\left((s - s_0)^{2q}\right). \tag{49}$$

The reduced-order model given by $\mathbf{Z}_n^{(\mathrm{Padé})}$ is passive for the special cases of RC, RL, and LC circuits (see [12, 13, 4]), however, for RLC circuits, it is not passive in general.

On the other hand, by applying the projection process described in Section 3, one can easily use the SyMPVL basis matrix $\mathbf{V}_n$ to generate an additional reduced-order model $\mathbf{Z}_n$ that is passive for general RLC circuits. Indeed, by (35), we simply need to compute the matrices

$$\mathbf{G}_n = \mathbf{V}_n^{\mathrm{T}}\,\mathbf{J}\,\mathbf{G}\,\mathbf{V}_n, \quad \mathbf{C}_n = \mathbf{V}_n^{\mathrm{T}}\,\mathbf{J}\,\mathbf{C}\,\mathbf{V}_n, \quad \mathbf{B}_n = \mathbf{V}_n^{\mathrm{T}}\,\mathbf{B}, \tag{50}$$

and then set

$$\mathbf{Z}_n(s) = \mathbf{B}_n^{\mathrm{T}}\,\left(\mathbf{G}_n + s\,\mathbf{C}_n\right)^{-1}\mathbf{B}_n. \tag{51}$$

Recall that the matrices $\mathbf{J}\,\mathbf{G}$ and $\mathbf{J}\,\mathbf{C}$ in (50) are given by (10). By Theorem 3, the reduced-order model $\mathbf{Z}_n$ given by (50) and (51) is passive. Moreover, by Theorem 2, $\mathbf{Z}_n$ still matches half as many moments as $\mathbf{Z}_n^{(\mathrm{Padé})}$, i.e.,

$$\mathbf{Z}_n(s) = \mathbf{Z}(s) + \mathcal{O}\left((s - s_0)^{q}\right). \tag{52}$$

Finally, by Theorem 1, the reduced-order model $\mathbf{Z}_n$ does not depend on the actual choice of the basis vectors for $\mathcal{K}_n(\mathbf{A}, \mathbf{R})$. Assuming that no deflation is necessary, PRIMA [16, 17] employs a block Arnoldi process to generate basis vectors for $\mathcal{K}_n(\mathbf{A}, \mathbf{R})$, and then uses the projection process described in Section 3 to obtain a reduced-order model. By Theorem 1, the PRIMA reduced-order model and the additional SyMPVL reduced-order model $\mathbf{Z}_n$ are identical.

5.3 Special Cases of RC, RL, and LC Circuits

For RC and RL circuits, the matrices $\mathbf{G}$ and $\mathbf{C}$ are symmetric positive semi-definite, and as a result, $\mathbf{J} = \mathbf{I}$ in (50). By (44) and (45), it thus follows that

$$\mathbf{G}_n + s_0\,\mathbf{C}_n = \mathbf{V}_n^{\mathrm{T}}\,\left(\mathbf{G} + s_0\,\mathbf{C}\right)\,\mathbf{V}_n = \mathbf{\Delta}_n \quad \text{and} \quad \mathbf{T}_n = \mathbf{\Delta}_n^{-1}\,\mathbf{C}_n. \tag{53}$$

Using (53), (50), and (47), we can rewrite the formula (51) of $\mathbf{Z}_n$ as follows:

$$\begin{aligned}\mathbf{Z}_n(s) &= \mathbf{B}_n^{\mathrm{T}}\,\left(\mathbf{G}_n + s_0\,\mathbf{C}_n + (s - s_0)\,\mathbf{C}_n\right)^{-1}\mathbf{B}_n \\ &= \left(\mathbf{\Delta}_n\,\boldsymbol{\rho}_n\right)^{\mathrm{T}}\,\left(\mathbf{I} + (s - s_0)\,\mathbf{T}_n\,\right)^{-1}\,\boldsymbol{\rho}_n.\end{aligned} \tag{54}$$

However, by (48), this is just the Padé approximant $\mathbf{Z}_n^{(\mathrm{Padé})}$. Therefore, for RC and RL circuits, the reduced-order models $\mathbf{Z}_n$ and $\mathbf{Z}_n^{(\mathrm{Padé})}$ are identical. In particular, this shows that PRIMA applied to RC circuits actually generates reduced-order models that match $2q$ moments, and not only q as stated in [17].

Finally, for LC circuits, one can show similarly that $\mathbf{Z}_n$ and $\mathbf{Z}_n^{(\mathrm{Padé})}$ are identical.

5.4 SyMPVL vs. PRIMA

For general RLC circuits, SyMPVL has the big advantage that it generates both the Padé-based reduced-order model $\mathbf{Z}_n^{(\text{Padé})}$, which in terms of moment matching has maximal possible accuracy, and the passive reduced-order model $\mathbf{Z}_n$ defined by projection. On the other hand, running PRIMA for the same number of steps only gives $\mathbf{Z}_n$. Furthermore, n steps of SyMPVL are always computationally less expensive than n steps of PRIMA. The Lanczos-type algorithm used in SyMPVL is also more general than the block Arnoldi process on which PRIMA is based, in that it allows for deflation of linearly dependent vectors, see [1, 13], while in PRIMA, it is simply assumed that deflation would never occur. There are two reasons for the computational savings of SyMPVL over PRIMA. First, SyMPVL requires the computation of a factorization of the symmetric matrix $\mathbf{G} + s_0\,\mathbf{C}$. This is only half as expensive as computing a factorization of the nonsymmetric matrix $\mathbf{J}\,\mathbf{G} + s_0\,\mathbf{J}\,\mathbf{C}$, which is required in PRIMA. Second, the length of the recurrences used to generate the Lanczos vectors in SyMPVL is at most 2m+1, while the length of the Arnoldi recurrences in PRIMA grows with the number n of basis vectors. As a result, the number of vector operations is less in SyMPVL than in PRIMA. Even if the Lanczos-type process in SyMPVL is run with full re-orthogonalization to eliminate possible convergence delay due to loss of orthogonality, the number of vector operations in SyMPVL is never higher than in PRIMA.

For RC, RL, and LC circuits, SyMPVL has the advantage that it directly generates the representation (48) of the reduced-order model $\mathbf{Z}_n^{(\text{Padé})} = \mathbf{Z}_n$. This saves the explicit computation of the projected matrices (50) that is required in PRIMA. Note that (50) involves n matrix-vector products with $\mathbf{G}$ and n matrix-vector products with $\mathbf{C}$.

6 Examples

In this section, we present two circuit examples.

6.1 A Package Model

The first example arises is the analysis of a 64-pin package model used for an RF integrated circuit. Only eight of the package pins carry signal, the rest being either unused or carrying supply voltages. The package is characterized as a 16-port component (8 exterior and 8 interior terminals). The package model is described by approximatively 4000 circuit elements, resistors, capacitors, inductors, and inductive couplings. The size of the nodal circuit matrices for the package is about 2000.

In [12], SyMPVL was used to compute a Padé-based reduced-order model of the package, and it was found that a model $\mathbf{Z}_n^{(\text{Padé})}$ of order $n = 80$ is sufficient to match the transfer-function components of interest. However, the model $\mathbf{Z}_n^{(\text{Padé})}$ has a few poles in the right half of the complex plane, and therefore, it is not passive.

In order to obtain a passive reduced-order model, we ran SyMPVL again on the package example, and this time, also generated the projected reduced-order model $\mathbf{Z}_n$. The expansion point $s_0 = 5\pi \times 10^9$ was used. Since $\mathbf{Z}_n$ is less accurate than $\mathbf{Z}_n^{(\text{Padé})}$, one now has to go to order $n = 112$ to obtain a reduced-order model that matches the transfer-function

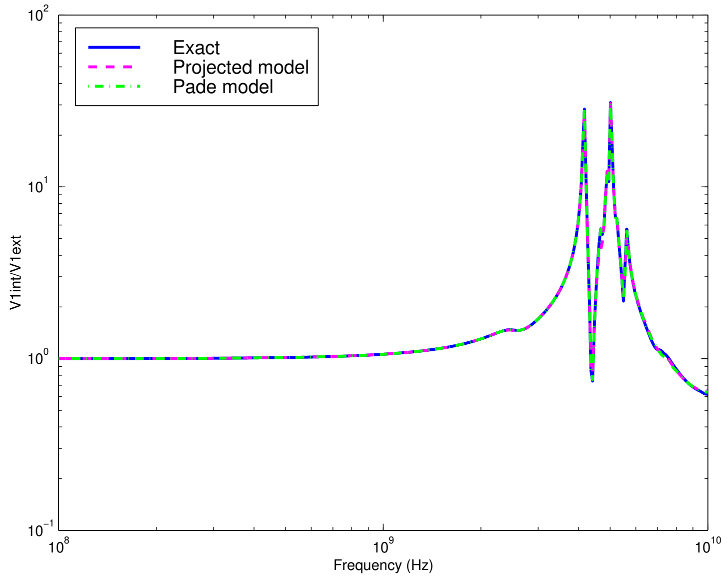

Figure 1: Package: Pin no.1 external to Pin no.1 internal, exact, projected model, and Padé model

components of interest. Figures 1 and 2 show the voltage-to-voltage transfer function between the external terminal of pin no. 1 and the internal terminals of the same pin and the neighboring pin no. 2, respectively. The plots show results with the projected model and the Padé model, both of order $n = 112$, compared with an exact analysis.

In Figure 3, we compare the relative error of the projected model $\mathbf{Z}_{112}$ and the Padé model $\mathbf{Z}_{112}^{(\text{Padé})}$ of the same size. Clearly, the Padé model is more accurate. However, out of the 112 poles of $\mathbf{Z}_{112}^{(\text{Padé})}$, 22 have positive real part, violating the passivity of the Padé model. On the other hand, the projected model is passive.

6.2 An Extracted RC Circuit

This is an extracted RC circuits with about 4000 elements and $m = 20$ ports. The expansion point $s_0 = 0$ was used. Since the projected model and the Padé model are identical for RC circuits, we only computed the Padé model via SyMPVL.

The point of this example is to illustrate the usefulness of the deflation procedure built into SyMPVL. It turned out that sweeps through the first two Krylov blocks, $\mathbf{R}$ and $\mathbf{A}\,\mathbf{R}$, of the block Krylov sequence (14) were sufficient to obtain a reduced-order model that matches the transfer function in the frequency range of interest. During the sweep through the second block, 6 almost linearly dependent vectors were discovered and deflated. As a result, the reduced-order model obtained with deflation is only of size $n = 2m - 6 = 34$. When SyMPVL was rerun on this example, with deflation turned off, a reduced-order model of size $n = 40$ was needed to match the transfer function. In Figure 4, we show the $Z_{1,11}$ component of the reduced-order model obtained with deflation and without deflation, compared to the exact transfer function. Clearly, deflation leads to a significantly smaller reduced-order model that is as accurate as the bigger one generated without deflation.

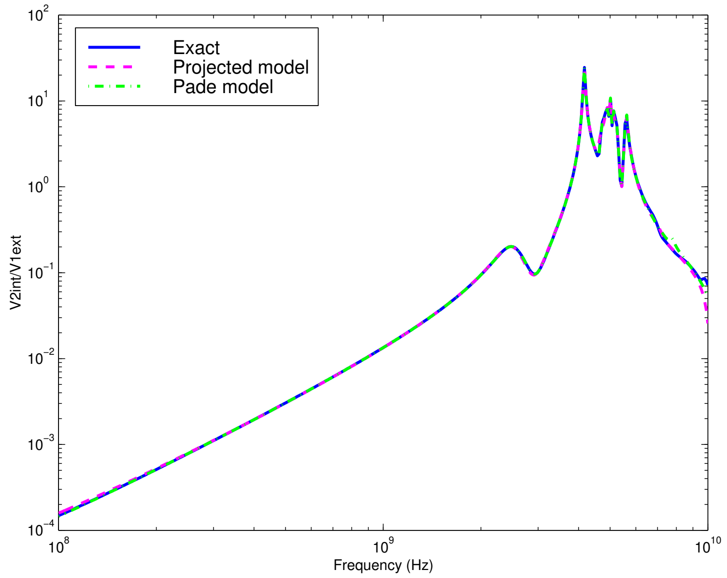

Figure 2: Package: Pin no.1 external to Pin no.2 internal, exact, projected model, and Padé model

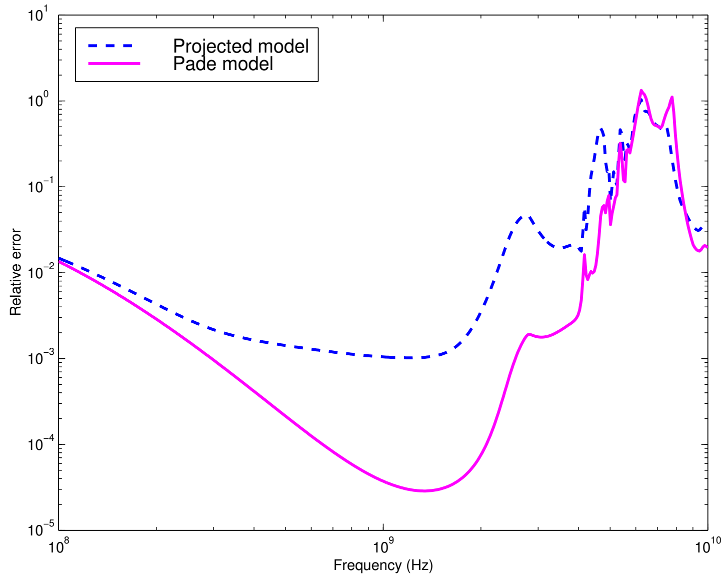

Figure 3: Relative error of projected model and Padé model

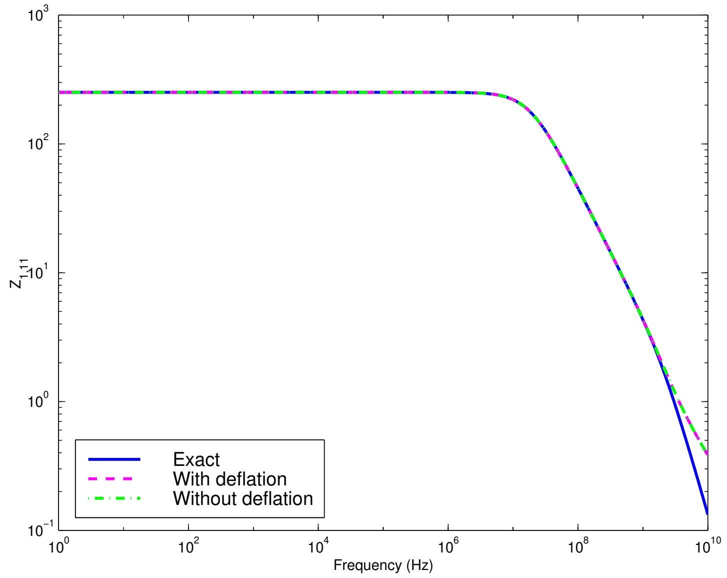

Figure 4: Impedance $Z_{1,11}$

7 Concluding Remarks

The results in this paper show that passive reduced-order models of RLC multi-ports can be obtained via a general projection technique based on block Krylov subspaces. The resulting reduced-order models are independent of the particular choice of basis vectors for the block Krylov subspaces, and thus they can be generated by means of any algorithm that generates suitable basis vectors for these subspaces. In particular, the projection technique can easily be incorporated into the SyMPVL algorithm to obtain guaranteed passive reduced-order models, in addition to the high-accuracy Padé-based reduced-order models, which may not be passive for general RLC circuits.

Acknowledgment

I would like to thank Peter Feldmann for his help with the numerical examples.

References

[1] J.I. Aliaga, D.L. Boley, R.W. Freund, and V. Hernández, "A Lanczos-type algorithm for multiple starting vectors," revised version, Numerical Analysis Manuscript No. 98–3–05, Bell Laboratories, Murray Hill, NJ, Sep. 1998.
Also available online from `http://cm.bell-labs.com/cs/doc/98`.

[2] B.D.O. Anderson and S. Vongpanitlerd, *Network Analysis and Synthesis*, Englewood Cliffs, NJ: Prentice-Hall, 1973.

[3] W.E. Arnoldi, "The principle of minimized iterations in the solution of the matrix eigenvalue problem," *Quart. Appl. Math.*, vol. 9, pp. 17–29, 1951.

[4] Z. Bai, P. Feldmann, and R.W. Freund, "How to make theoretically passive reduced-order models passive in practice," In *Proc. IEEE 1998 Custom Integrated Circuits Conference*, IEEE, May 1998.

[5] G.A. Baker, Jr. and P. Graves-Morris, *Padé Approximants*, Second Edition, New York, NY: Cambridge University Press, 1996.

[6] I.M. Elfadel and D.D. Ling, "Zeros and passivity of Arnoldi-reduced-order models for interconnect networks," in *Proc. 34nd ACM/IEEE Design Automation Conf.*, Jun. 1997.

[7] P. Feldmann and R.W. Freund, "Efficient linear circuit analysis by Padé approximation via the Lanczos process," *IEEE Trans. Computer-Aided Design*, vol. 14, pp. 639–649, May 1995.

[8] P. Feldmann and R.W. Freund, "Reduced-order modeling of large linear subcircuits via a block Lanczos algorithm," in *Proc. 32nd ACM/IEEE Design Automation Conf.*, June 1995.

[9] P. Feldmann and R.W. Freund, Interconnect-delay computation and signal-integrity verification using the SyMPVL algorithm, in *Proc. 1997 European Conference on Circuit Theory and Design*, European Circuit Society, Sep. 1997.

[10] R.W. Freund, "Computation of matrix Padé approximations of transfer functions via a Lanczos-type process," in *Approximation Theory VIII, Vol. 1: Approximation and Interpolation*, C.K. Chui and L.L. Schumaker, eds., World Scientific Publishing Co., 1995.

[11] R.W. Freund and P. Feldmann, "Reduced-order modeling of large passive linear circuits by means of the SyPVL algorithm," in *Tech. Dig. 1996 IEEE/ACM International Conference on Computer-Aided Design*, Nov. 1996.

[12] R.W. Freund and P. Feldmann, "The SyMPVL algorithm and its applications to interconnect simulation," in *Proc. 1997 International Conference on Simulation of Semiconductor Processes and Devices*, IEEE, Sep. 1997.

[13] R.W. Freund and P. Feldmann, "Reduced-order modeling of large linear passive multi-terminal circuits using matrix-Padé approximation," in *Proc. Design, Automation and Test in Europe Conference 1998*, IEEE Computer Society Press, Feb. 1998.

[14] K.J. Kerns and A.T. Yang, "Preservation of passivity during RLC network reduction via split congruence transformations," in *Proc. 34nd ACM/IEEE Design Automation Conf.*, 1997.

[15] C. Lanczos, "An iteration method for the solution of the eigenvalue problem of linear differential and integral operators," *J. Res. Nat. Bur. Standards*, vol. 45, pp. 255–282, 1950.

[16] A. Odabasioglu, Provably passive RLC circuit reduction, M.S. thesis, Carnegie Mellon University, Pittsburgh, Pennsylvania, 1996.

[17] A. Odabasioglu, M. Celik, L.T. Pileggi, "PRIMA: passive reduced-order interconnect macromodeling algorithm," in *Tech. Dig. 1997 IEEE/ACM International Conference on Computer-Aided Design*, Nov. 1997.

[18] L.T. Pillage and R.A. Rohrer, "Asymptotic waveform evaluation for timing analysis," *IEEE Trans. Computer-Aided Design*, vol. 9, pp. 352–366, Apr. 1990.

[19] V. Raghavan, R.A. Rohrer, L.T. Pillage, J.Y. Lee, J.E. Bracken, and M.M. Alaybeyi, "AWE–inspired," in *Proc. IEEE Custom Integrated Circuits Conference*, May 1993.

[20] A. Ruhe, "Implementation aspects of band Lanczos algorithms for computation of eigenvalues of large sparse symmetric matrices," *Math. Comp.*, vol. 33, pp. 680–687, 1979.

[21] L.M. Silveira, M. Kamon, I. Elfadel, and J. White, "A coordinate-transformed Arnoldi algorithm for generating guaranteed stable reduced-order models of RLC circuits," in *Tech. Dig. 1996 IEEE/ACM International Conference on Computer-Aided Design*, Nov. 1996.

[22] J. Vlach and K. Singhal, *Computer Methods for Circuit Analysis and Design*, Second Edition, New York, N.Y.: Van Nostrand Reinhold, 1993.

[23] M.R. Wohlers, *Lumped and Distributed Passive Networks*, New York, N.Y.: Academic Press, 1969.

Appendix

In this appendix, we establish the relations (33) and (34), which were used in the proof of Theorem 2.

Recall from (20) and (21) that the columns of the matrix $\mathbf{V}_n$ span the n-th block Krylov subspace $\mathcal{K}_n(\mathbf{A}, \mathbf{R})$. Together with the definition of $\mathcal{K}_n(\mathbf{A}, \mathbf{R})$ in Section 3.1, it follows that for each $i = 1, 2, \ldots, q$, there exists an $n \times m$ matrix $\mathbf{E}_i$ such that

$$\mathbf{A}^{i-1}\,\mathbf{R} = \mathbf{V}_n\,\mathbf{E}_i. \tag{55}$$

Proof of Equation (33)

By (13) and (55) (for i=1), we have

$$\mathbf{B} = (\mathbf{G} + s_0\,\mathbf{C})\ \mathbf{R} = (\mathbf{G} + s_0\,\mathbf{C})\ \mathbf{V}_n\,\mathbf{E}_1 = (\mathbf{G}\,\mathbf{V}_n + s_0\,\mathbf{C}\,\mathbf{V}_n)\ \mathbf{E}_1. \tag{56}$$

Multiplying (56) from the left by $\mathbf{V}_n^{\mathrm{H}}$ and using (23), we obtain the relation

$$\mathbf{B}_n = (\mathbf{G}_n + s_0\,\mathbf{C}_n)\ \mathbf{E}_1,$$

or, equivalently,

$$(\mathbf{G}_n + s_0\,\mathbf{C}_n)^{-1}\,\mathbf{B}_n = \mathbf{E}_1. \tag{57}$$

Multiplying the equation for $\mathbf{F}$ in (32) from the right by $\mathbf{V}_n$, and using the equation for $\mathbf{C}_n$ in (23), we get

$$\mathbf{F}\,\mathbf{V}_n = \mathbf{V}_n\ (\mathbf{G}_n + s_0\,\mathbf{C}_n)^{-1}\ \mathbf{C}_n.$$

This relation, by induction on i, implies that

$$\mathbf{F}^i\,\mathbf{V}_n = \mathbf{V}_n\ \left((\mathbf{G}_n + s_0\,\mathbf{C}_n)^{-1}\,\mathbf{C}_n\right)^i \quad \text{for all} \quad i = 0, 1, \ldots\ . \tag{58}$$

Note that, by (23), $\mathbf{L}_n^{\mathrm{H}} = \mathbf{L}^{\mathrm{H}}\,\mathbf{V}_n$. Using this relation, as well as (30), (57), (58), and (55) (for i=1), we obtain, for all $i = 0, 1, \ldots,$

$$\begin{aligned}
\widehat{\mathbf{M}}_i &= \mathbf{L}_n^{\mathrm{H}}\ \left((\mathbf{G}_n + s_0\,\mathbf{C}_n)^{-1}\,\mathbf{C}_n\right)^i\ (\mathbf{G}_n + s_0\,\mathbf{C}_n)^{-1}\,\mathbf{B}_n \\
&= \mathbf{L}^{\mathrm{H}}\ \left(\mathbf{V}_n\left((\mathbf{G}_n + s_0\,\mathbf{C}_n)^{-1}\,\mathbf{C}_n\right)^i\right)\ \left((\mathbf{G}_n + s_0\,\mathbf{C}_n)^{-1}\,\mathbf{B}_n\right) \\
&= \mathbf{L}^{\mathrm{H}}\ \left(\mathbf{F}^i\,\mathbf{V}_n\right)\ \mathbf{E}_1 \\
&= \mathbf{L}^{\mathrm{H}}\,\mathbf{F}^i\,\mathbf{R},
\end{aligned}$$

which is just the desired relation (33).

Proof of Equation (34)

The proof is by induction on i. For $i = 0$, (34) is trivially satisfied. Now assume that (34) is true for some $0 \le i < q - 1$. We show that (34) then also holds true for $i + 1$, i.e.,

$$\mathbf{F}^{i+1}\,\mathbf{R} = \mathbf{A}^{i+1}\,\mathbf{R}. \tag{59}$$

Using (13), (34), and (55) (with i replaced by $i + 1$), we get

$$\left((\mathbf{G} + s_0\,\mathbf{C})^{-1}\,\mathbf{C}\right)\ \left(\mathbf{F}^i\,\mathbf{R}\right) = \mathbf{A}\ \left(\mathbf{A}^i\,\mathbf{R}\right) = \mathbf{A}^{i+1}\,\mathbf{R} = \mathbf{V}_n\,\mathbf{E}_{i+1}. \tag{60}$$

Multiplying (60) from the left by $\mathbf{V}_n^{\mathrm{H}}\ (\mathbf{G} + s_0\,\mathbf{C})$, it follows that

$$\left(\mathbf{V}_n^{\mathrm{H}}\,\mathbf{C}\right)\ \left(\mathbf{F}^i\,\mathbf{R}\right) = \left(\mathbf{V}_n^{\mathrm{H}}\ (\mathbf{G} + s_0\,\mathbf{C})\ \mathbf{V}_n\right)\ \mathbf{E}_{i+1}. \tag{61}$$

Note that, by (23), $\mathbf{V}_n^{\mathrm{H}}\ (\mathbf{G} + s_0\,\mathbf{C})\ \mathbf{V}_n = \mathbf{G}_n + s_0\,\mathbf{C}_n$. Using this relation, as well as (32) and (55) (with i replaced by $i + 1$), we obtain from (61) that

$$\mathbf{F}^{i+1}\,\mathbf{R} = \mathbf{F}\ \left(\mathbf{F}^i\,\mathbf{R}\right) = \mathbf{V}_n\ \left((\mathbf{G}_n + s_0\,\mathbf{C}_n)^{-1}\,\mathbf{V}_n^{\mathrm{T}}\,\mathbf{C}\right)\ \left(\mathbf{F}^i\,\mathbf{R}\right) = \mathbf{V}_n\,\mathbf{E}_{i+1} = \mathbf{A}^{i+1}\,\mathbf{R},$$

which is just the desired relation (59).